Available online at www.sciencedirect.com
ScienceDirect
Quaternary Research 69 (2008) 231–241
QUATERNARY RESEARCH
www.elsevier.com/locate/yqres

Exposure age chronology of the last glaciation in the eastern Pyrenees

Magali Delmas [a,b], Yanni Gunnell [b,*], Régis Braucher [c], Marc Calvet [a], Didier Bourlès [c]

[a] Médi-Terra, Université de Perpignan, 52 av. Paul Alduy, 66860 Perpignan, France
[b] UMR CNRS 8591, Université de Paris 7, Case 7001, 2 place Jussieu, 75251 Paris cedex 05, France
[c] CEREGE, CNRS UMR 6635, BP 80, 13545 Aix-en-Provence cedex 04, France

Received 7 October 2006
Available online 10 March 2008

Abstract

We present a chronology of ice recession in the eastern Pyrenees based on *in situ*-produced ^{10}Be data obtained from the Têt paleoglacier complex. The sampling strategy is based on the relative chronology provided by a detailed geomorphological map of glacial landforms. Results indicate that the last maximum ice advance occurred late (i.e., during Marine Isotope Stage 2) compared to the chronology currently established for the rest of the Pyrenees. Despite debatable evidence for a glacial readvance during the Oldest Dryas stade, ice-cap melt-out was rapid, residual cirque glaciers having disappeared by the Allerød interstade. This is consistent both with North Atlantic excursions established by the Greenland ice cores and paleoenvironmental data for the region. The rapid response of the east-Pyrenean ice cap to temperature variations is primarily linked to its small size compared to larger Pyrenean ice fields, to the dry Mediterranean climate, and to topography-related nonlinearities in which a small vertical rise in equilibrium line altitude generates a large change in ice mass. Possible sources of age uncertainty are discussed in the context of sampling design for single-nuclide (^{10}Be) dating of landform sequences in formerly glaciated landscapes.

Keywords: Last Pleistocene glacial cycle; Deglaciation chronology; Geomorphological mapping; Beryllium exposure dating; Radiocarbon dating; Pyrenees

Introduction

Maximum ice extent (MIE) refers to the farthest advance of ice out of a mountain crest zone. Existing chronologies of the last glaciation in the Pyrenees indicate that the MIE of the last Pleistocene glacial cycle occurred earlier than the global last glacial maximum (LGM) of Marine Isotope Stage 2 (MIS 2). On the north side of the range, this is based on a series of radiocarbon ages obtained from glacio-lacustrine sediments contained behind MIE moraines (Fig. 1: Mardonnes and Jalut, 1983; Andrieu, 1987; Andrieu et al., 1988; Jalut et al., 1988, 1992). These piedmont sites show that ice positions were stable until 29,500 ± 1200 (Gif-5683) ^{14}C yr BP in the Gave de Pau catchment (Biscaye borehole) and 24,400 ± 1000 (Gif-6867) ^{14}C yr BP in the Gave d'Ossau catchment (Estarres borehole) only a few kilometers upstream from the outermost terminal moraines of the MIE. Accelerated ice retreat at those western sites occurred soon after those dates, and is recorded from 26,600 ± 460 (TAN-82282) ^{14}C yr BP on the Garonne river (Barbazan borehole). An early occurrence of both the MIE and the beginning of deglaciation are also confirmed on the Garonne glacier by pollen spectra (Sost lake: Hérail and Jalut, 1986). In the Ariège river catchment, the uranium-series-dated Niaux–Lombrives stalagmitic floor is 19–20 ka and seals glacial outwash deposits (Soriaux, 1981; Bakalowicz et al., 1984). Cessation of glacio-lacustrine sedimentation at the elevated sites of Bious (1550 m a.s.l.) and Freychinèdes (1350 m a.s.l.) also indicates that glaciers were essentially confined to cirques after 15,800 ± 240 (Gif-7078) and 14,700 ± 800 (Gif-5018) ^{14}C yr BP, respectively. This correlates with a sharp rise in drought-tolerant taxa in all pollen diagrams of the alpine vegetation zones (Andrieu et al., 1988). This cirque stage ('stade des cirques' of Viers, 1968), so named because it reflects the residual stages of glaciation in the Pyrenees, generated well-preserved moraine complexes. It was also termed 'Neoglacial' by Taillefer (1969), who suggested a glacial readvance. However, apart from a few localized sites where glaciers still occur today (Chueca Cía et al., 2004; Gellatly et al., 1992), details of latest Pleistocene stages remain poorly defined.

* Corresponding author.
E-mail address: gunnell@univ-paris-diderot.fr (Y. Gunnell).

0033-5894/$ - see front matter © 2008 University of Washington. All rights reserved.
doi:10.1016/j.yqres.2007.11.004

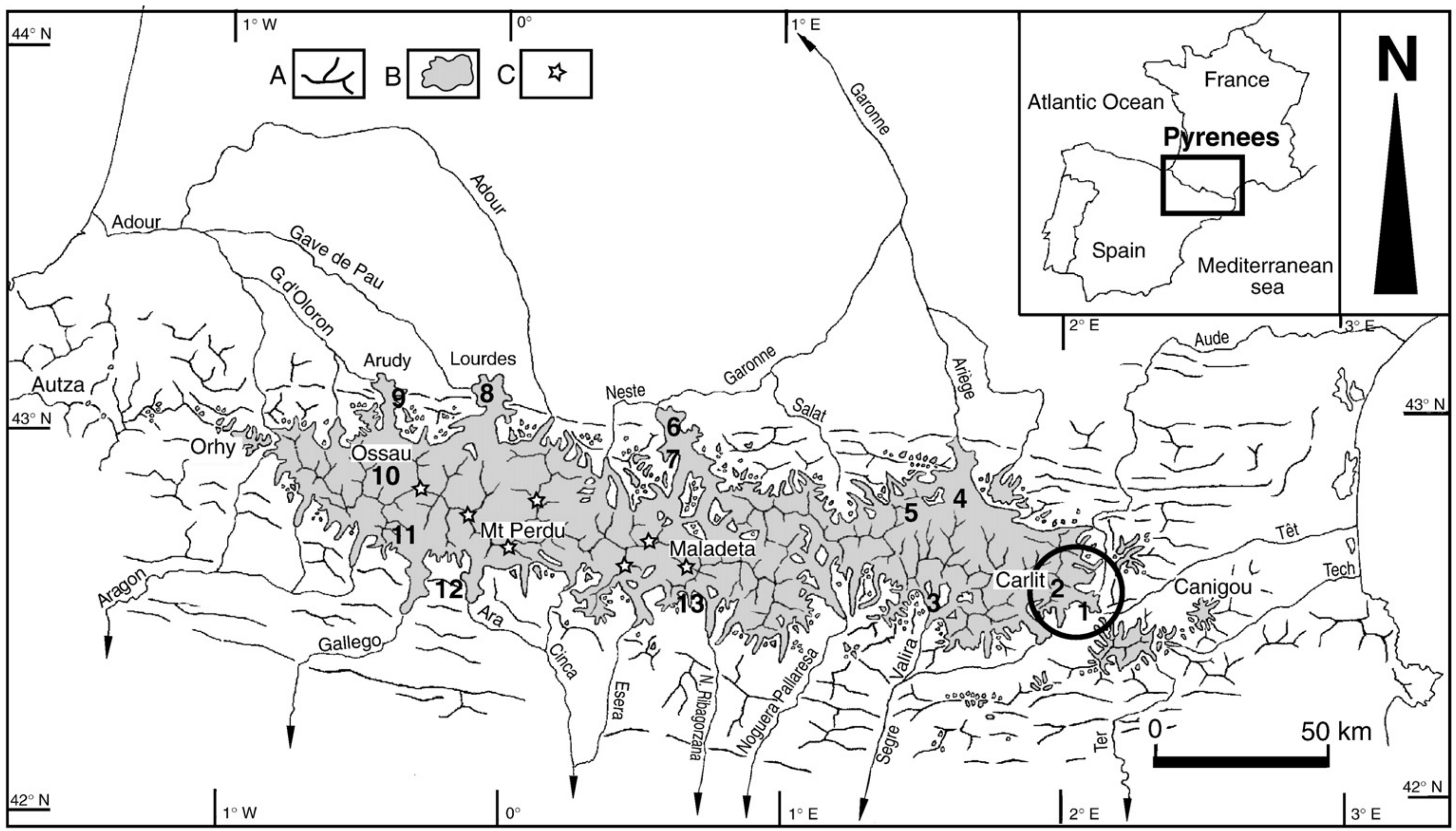

Figure 1. Maximum ice extent in the Pyrenees during the last glacial cycle (modified from Calvet, 2004). Key to locations mentioned in text: 1: La Borde and Le Racou. 2: La Grave-amont. 3: Arinsal (Andorre). 4: Niaux–Lombrives (Tarascon, Ariège). 5: Freychinèdes. 6: Barbazan. 7: Sost. 8: Biscaye. 9: Estarrès, Castet. 10: Bious. 11: Tramacastilla, Formigal, Portalet. 12: Linas de Broto. 13: Llestui. A: main topographic ridge lines. B: MIE ice field. C: massifs with surviving glaciers in the present day.

https://doi.org/10.1016/j.yqres.2007.11.004 Published online by Cambridge University Press

The chronology of the last glacial cycle on the south Pyrenean mountain front, also mostly indexed on radiocarbon ages, broadly matches findings obtained in the north. The early occurrence of the MIE on the Noguera Ribagorçana valley (Vilaplana, 1983; Vilaplana and Bordonau, 1989) is corroborated by recent OSL ages on glacio-fluvial terraces and terminal moraines of the Cinca (Sancho et al., 2003) and Gallego (Peña et al., 2004) rivers. On the Ara river, the 60 m-thick kame terrace of Llinas de Broto has yielded an AMS age of 30,380±400 (AZ-35868) ^{14}C yr BP at 22 m from the base (Martí-Bono et al., 2002). As in the north, early deglaciation is supported by 29,400±600 (Gif-8239) to 21,970±200 (Gif-8258) ^{14}C yr BP sediment ages in the proglacial lake at Tramacastilla (upper Gallego basin), and in two peat bogs near the Pourtalet mountain pass (20,150±150 (AZ-35867) ^{14}C yr BP and 28,300±370 (NSRL-11969) ^{14}C yr BP, respectively: Garcia-Ruiz et al., 2003; González-Sampériz et al., 2006). This also concurs with data from the Cantabrian Mountains (Jiménez-Sánchez et al., 2002). Farther east, in Andorra, the delta and lake stratigraphy of the upper Arinsal valley has yielded ages ranging up-profile from 25,630±190 (β-115017) to 17,430±140 (β-115016) ^{14}C yr BP, suggesting an early severance of the Valira ice tongue from its tributaries (Turu i Michels, 2002). In summary, even though some radiocarbon ages are suspiciously old due to possible graphite contamination by Paleozoic schist outcrops (Bordonau i Ibern, 1992; Bordonau et al., 1993; Pallàs et al., 2006), or because AMS dating of single pollen grains cannot rule out that the grains are reworked from an older deposit (Reille and Lowe, 1993; Reille and Andrieu, 1995), orogen-scale chronologies of the MIE from both sides of the mountain belt are currently in remarkably good agreement.

Geomorphic setting and cosmogenic nuclide exposure dating method

Relative chronology based on geomorphologic mapping

The Têt River flows to the Mediterranean Sea and the Pleistocene Têt glacier remained contained in the uppermost section of this now entirely deglaciated fluvial catchment (Fig. 2). Given that landforms and deposits from the last glaciation are remarkably well preserved, this area forms an ideal laboratory for studying the stages of glacial retreat using cosmogenic radionuclide dating (CRN). Up to eight stages of glacier recession have been mapped (Fig. 3). During the MIE (Fig. 4a), the massif was covered by an ice cap, with few nunataks and 300-m-thick valley ice flowing south. Geometric relationships between recessional and lateral moraines show that ice had thinned by the time of the Borde stage (Fig. 4b). This caused a fragmentation of the ice cap into several tongues separated by ice-free embayments at 2.2 km a.s.l. The accumulation zones were nevertheless sufficiently well supplied for the main Têt glacier tongue to extend to within only 2–3 km from the MIE terminal moraines. Decay of the ice cap proceeded through successive break-up stages (Fig. 4c to e), finally attaining the cirque stage (Fig. 4f). This involved active cirque glaciers facing north, east and southeast with a record of up to 4 recessional moraines.

CRN sampling strategy

Compared with the potential for radiocarbon dating in deglaciated areas, which must focus on post-glacial or interglacial organic-sediment traps, CRN presents the advantage of allowing

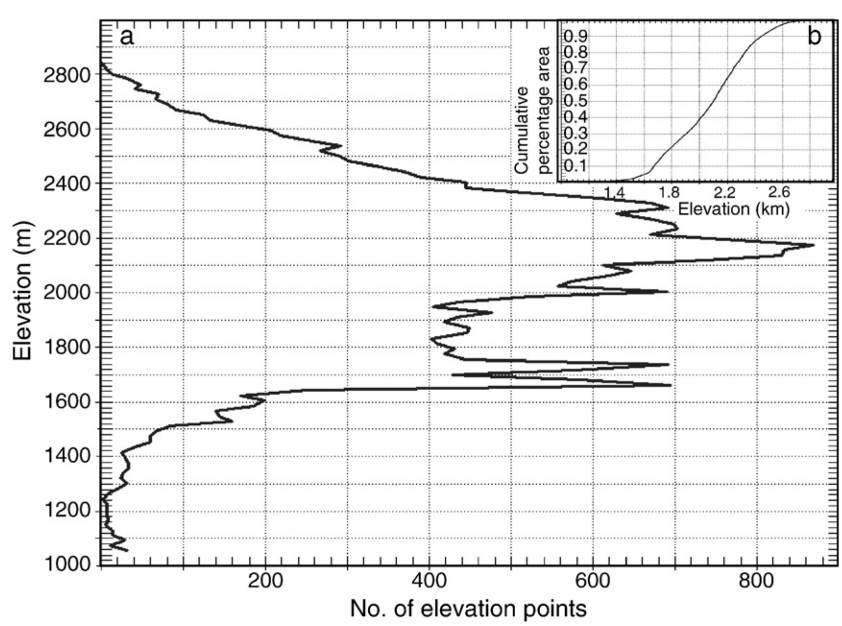

Figure 2. Hypsometry of the upper Têt basin. a: hypsometric curve; b: hypsometric integral. Data derived from Shuttle Radar Topography Mission 90-m digital elevation map. Note the wide extent of plateau topography between 2000 and 2400 m a.s.l. and limited residual surface area above that threshold, with implications for rapid ice cap recession for small increments in upward ELA migration.

https://doi.org/10.1016/j.yqres.2007.11.004 Published online by Cambridge University Press

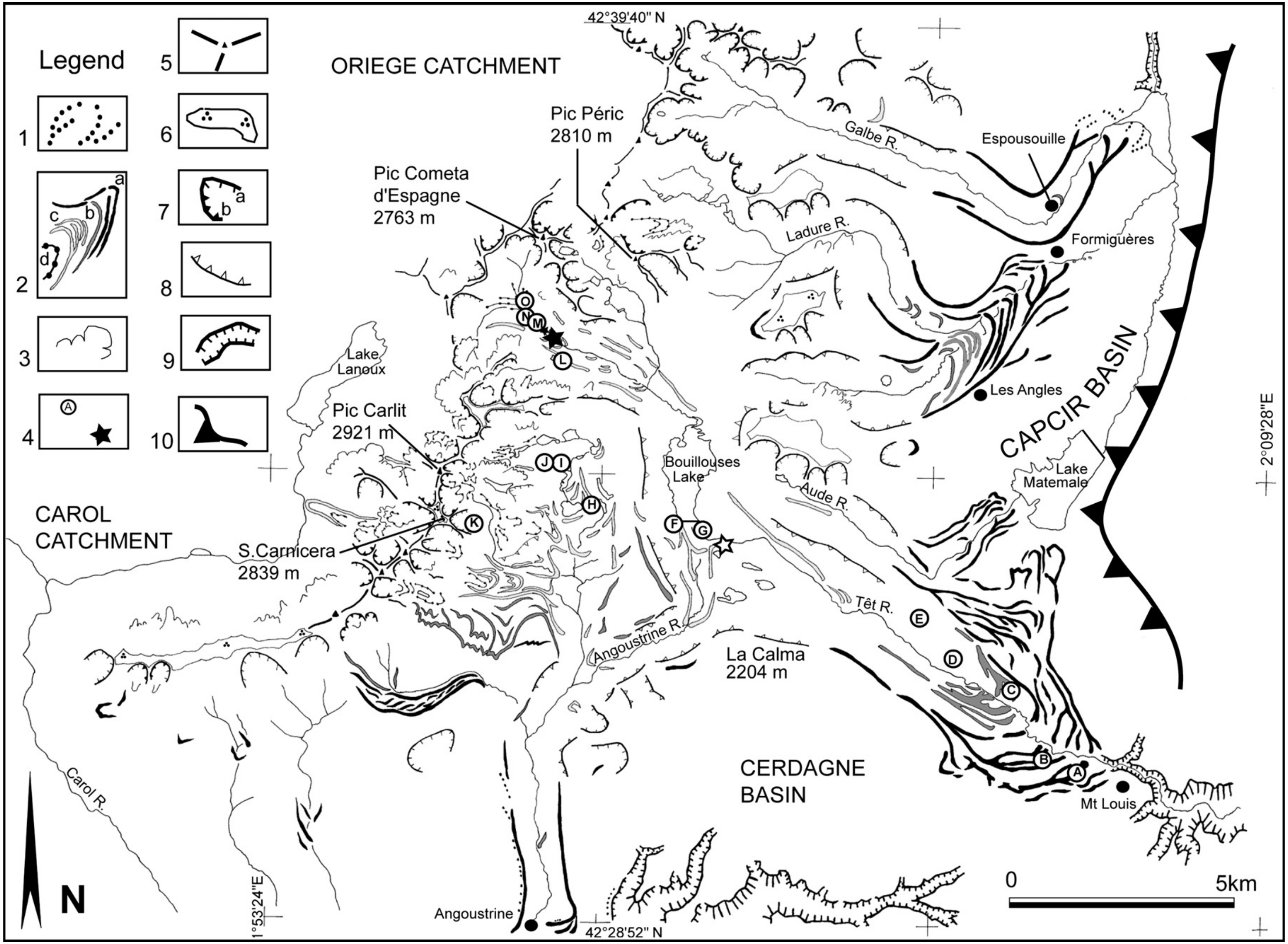

Figure 3. Geomorphological map and relative chronology of glacial landforms. Key to symbols: 1: pre-Würm moraines. 2: moraines from the last glacial cycle (a: MIE; b: Borde stage; c: break-up stages; d: cirque stage). 3: rock glaciers. 4: ^{10}Be sampling sites (circled letters), radiocarbon-dated Grave-amont (black star) and Racou (open star) sites after Guiter et al. (2005). 5: topographic ridge lines and main summits. 6: non-glaciated surfaces exhibiting marks of frost action. 7: scree-covered (a) and bedrock (b) cirque walls. 8: main glacial trough walls. 9: fluvial incision. 10: west-facing faceted fault scarp on east side of Capcir half-graben.

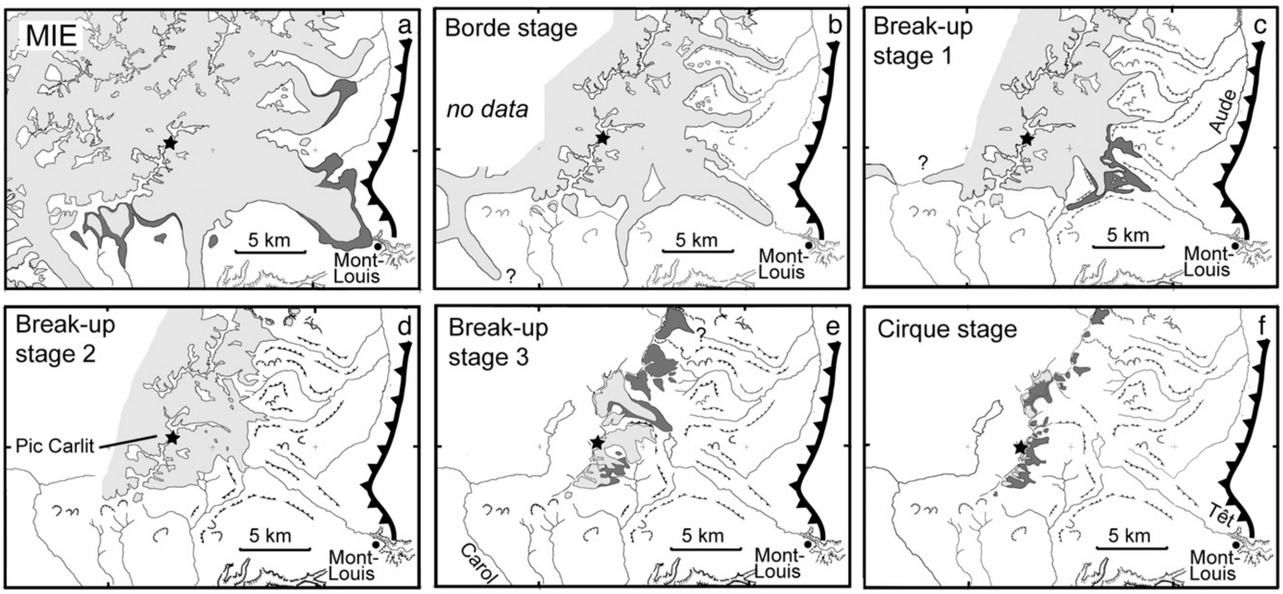

Figure 4. Reconstruction of the Carlit ice cap at successive recessional stages (a to f) based on detailed geomorphological mapping from aerial photographs and field reconnaissance. Symbols, ornaments and lat/long tick marks as in Figure 3. At each stage, dark gray and light gray shading define the uncertainty of glacier extent (i.e., maximum and minimum position of ice fronts, respectively) linked to the mapping method.

glacial landforms to be sampled directly. Furthermore, it becomes possible to track the geomorphic sequence from MIE terminal moraines to the cirques, and thus reconstruct the last glacial cycle. Ideally (i.e., irrespective of local-scale environmental factors which we discuss later), the concentration of *in situ*-produced ^{10}Be in a rock is a function of exposure time to cosmic rays after the rock has reached the surface, ^{10}Be production rate at the site, radioactive decay of the isotope, and the erosion rate of the rock surface. We therefore targeted rock surfaces that had suffered no detectable post-glacial degradation by erosion in order that CRN exposure ages could be calculated under the key assumption of no denudation. Scour-marked bedrock steps in the longitudinal valley profile, which are typically sculpted into *roches moutonnées*, were the best candidates. However, near the glacier snouts, moraine ridges were the best landforms available. On erratic boulders, fresh rock faces devoid of detectable chemical degradation and spalling were sampled. Overall, the study covers 15 such sites partitioned between moraine ridges and glacially scoured rock exposures while ensuring that the MIE and most recession stages were documented (Figs. 3 and 5).

CRN exposure ages on bedrock exposures indicate time since vacation by ice. The spatially averaged glacial erosion depth in the Têt catchment, calculated volumetrically from mapped moraine deposits, is ~5 m for the last glacial cycle. This is a minimal estimate because glaciers typically discharge

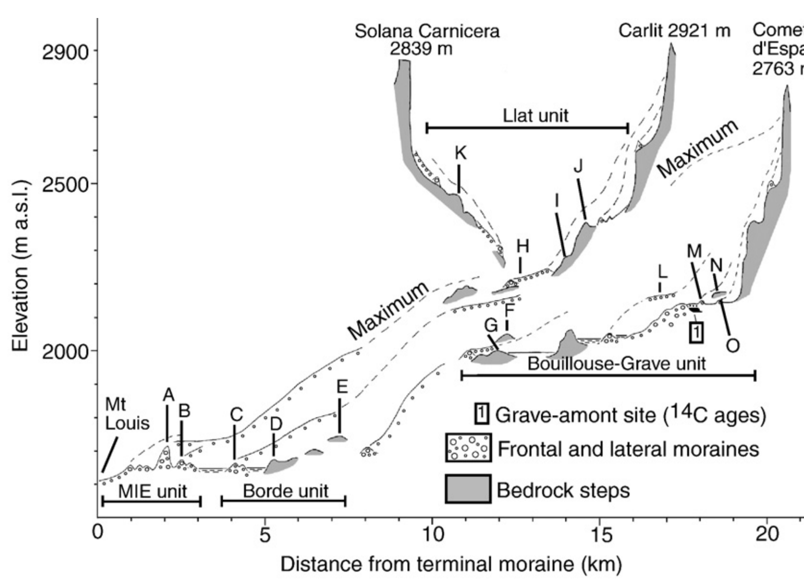

Figure 5. Partly schematic cross-section of glacial landforms along transect. Sampling sites are indicated A to O. Dashed lines in the sky define approximate ice thickness envelopes based on height of moraines mapped in Figure 3.

https://doi.org/10.1016/j.yqres.2007.11.004 Published online by Cambridge University Press

most of their sediment load in the finer fraction. The depth of bedrock erosion during that cycle was therefore sufficient that no inherited ^{10}Be should have accumulated from previous exposure intervals. In addition to this assumption, sample sites were collected along the axis of the major ice ways, where the erosional potential was highest. Together, these precautions limited risks of bias due to inherited nuclides. The samples were collected from the flatter tops of bedrock exposures sculpted by moving ice, where topographic shielding from cosmic rays is minimal. However, at such sites, a risk also occurs of scoured surface having been covered by till after ice melt-out, in which case the exposure age would indicate a younger event corresponding to the removal of the till cover by erosion.

Ages on boulders capping moraine ridge crests theoretically provide the age of the glacial stage responsible for moraine accumulation (Zreda and Phillips, 1994). However, the unconsolidated nature of moraine deposits exposes sampling to the likelihood of dating formerly buried boulders that have been exposed by post-depositional erosion. Putkonen and Swanson (2003) have studied the statistical risk of dating moraines and show that a 38% difference in exposure age can exist between the youngest and oldest boulders of a single moraine landform. They recommended a minimum sample of 6 to 7 boulders per landform for taller and older moraines (40–100 ka and 50–100 m high), and 1 to 4 boulders for lower ones (10–20 m high). Here, those guidelines were observed, with 2 to 3 replicates on moraine crests 10–15 m high. Only 3 samples were collected from the 100-m-high terminal moraine (site A), but this is compensated by the fact that sites A and B represent the same glacial stage and should yield indistinguishable ages. The flat upper surfaces of untilted summit boulders 3–5 m in diameter were targeted. As a safeguard against the risk of nuclide inheritance, the erratic boulder showing signs of having lost mass by rounding during transport was preferred. Due to the likely risk of post-depositional ridge erosion, the older age or ages obtained were considered to be closest to the true age of the landform (Putkonen and Swanson, 2003).

Distant shielding from surrounding topography and local shielding on sloping sampling surfaces were measured systematically using a compass and inclinometer, and corrected after Dunne et al. (1999). Shielding by snow at these altitudes also reduces the production rate of cosmogenic nuclides, and results in underestimates of exposure ages. Based on historic records, correction for snow cover was systematically applied. A mean value of 50 cm of snow cover (density 0.28) for 6 months of the year was assumed. However, we emphasize that historic records are generally limited to a few decades, and therefore data are unlikely to fully reflect the range of snow cover conditions over exposure periods of thousands of years (Schildgen et al., 2005). The applied correction implies less than 5% change in production rate derived from Stone polynomials (Stone, 2000).

Analytical procedure

Quartz was isolated from crushed and sieved samples of granite or vein quartz in micaschist by dissolving all other

Table 1
Cosmogenic ^{10}Be surface exposure data in the eastern Pyrenees (Têt ice cap)

Site			Sample	Position		Elevation	Production rate	[^{10}Be]	^{10}Be apparent exposure age
Unit	Sample Number		Type	Latitude	Longitude	(m a.s.l.)	(atom/g/year)	$*10^5$ (atom/g)	$*10^3$(year)
MIE	A	A1	Moraine boulder	42°30′32.6″	2°05′47.4″	1711	19.21	2.28±0.25	13.6±1.7
		A2	Moraine boulder	42°30′31.1″	2°05′37.5″	1700	19.07	2.86±0.62	17.2±3.9
		A3	Moraine boulder	42°30′30″	2°05′28.6″	1700	19.07	3.55±0.58	21.4±3.7
	B	B1	Moraine boulder	42°30′47.5″	2°05′38.3″	1670	18.64	2.65±0.45	16.3±2.9
		B2	Moraine boulder	42°30′48.1″	2°05′41″	1670	18.64	2.22±0.3	13.6±2
		B3	Moraine boulder	42°30′48.4″	2°05′43.1″	1670	18.51	2.21±0.28	13.7±1.9
Borde	C	C1	Moraine boulder	42°31′36.8″	2°05′19.3″	1655	18.46	3.03±0.39	18.9±2.7
		C2	Moraine boulder	42°31′32.7″	2°05′21.9″	1655	18.46	2.83±0.61	17.6±3.9
		C3	Moraine boulder	42°31′43.7″	2°05′17″	1655	18.46	3.29±0.49	20.5±3.3
	D	D1	Scoured rock	42°31′54.4″	2°04′38.3″	1680	18.80	3.92±0.76	24.0±4.9
	E	E1	Scoured rock	42°32′29″	2°03′27.1″	1750	20.25	3.26±0.57	18.5±3.4
Bouillouse-Grave	F	F1	Scoured rock	42°33′41.4″	1°59′38.6″	2085	24.76	2.91±0.4	13.5±2
	L	L1	Moraine boulder	42°35′39.6″	1°57′45.5″	2180	24.90	2.76±0.27	12.7±1.4
	M	M1	Moraine boulder	42°35′52.6″	1°57′41.2″	2150	24.36	2.54±0.38	11.9±1.9
		M2	Moraine boulder	42°35′52.8″	1°57′34.6″	2150	24.10	2.79±0.38	13.3±2
	N	N	Scoured rock	42°36′03.9″	1°57′18.4″	2170	24.90	2.71±0.34	12.5±1.7
	O	O2	Moraine boulder	42°36′09.1″	1°57′17.7″	2160	24.56	2.41±0.37	11.2±1.9
Llat	H	H1	Moraine boulder	42°33′46.2″	1°58′21.1″	2180	26.78	2.51±0.3	10.7±1.4
		H2	Moraine boulder	42°33′49.3″	1°58′21.2″	2180	26.78	4.17±0.51	17.8±2.4
		H3	Moraine boulder	42°33′41″	1°58′26.1″	2170	26.60	2.55±0.37	11.0±1.7
	I	I1	Scoured rock	42°34′22.6″	1°57′55.4″	2260	26.58	5.76±0.96	24.9±4.4
		I1bis[a]	Scoured rock	42°34′22.6″	1°57′55.4″	2260	26.58	5.62±0.93	24.3± 4.9
		I2	Scoured rock	42°34′19.4″	1°57′50.4″	2270	26.76	5.56±0.84	23.9±3.9
	J	J1	Scoured rock	42°34′19″	1°57′30.3″	2350	28.20	3.37±0.46	13.7±2
		J2	Scoured rock	42°34′14.7″	1°57′27.3″	2385	28.78	3.81±0.46	15.2±2
	K	K1	Scoured rock	42°33′38.3″	1°56′41.8″	2410	28.78	3.69±0.59	14.7±2.5

[a]I1bis is a replicate of I1.

https://doi.org/10.1016/j.yqres.2007.11.004 Published online by Cambridge University Press

minerals with mixtures of HCl and H_2SiF_6. Meteoric ^{10}Be was then eliminated by successive HF sequential dissolutions. The purified 0.25–1 mm granulometric quartz fraction was dissolved in Suprapur HF and the resulting solution spiked with 0.3 mg of ^{9}Be carrier. Beryllium was separated from these solutions by successive solvent extractions and precipitations. All ^{10}Be measurements were performed by accelerator mass spectrometry (AMS) at the Tandétron facility of Gif-sur-Yvette (France). Isotopic ratios were normalized to the National Institute Standards and Testing (NIST) Reference Material 4325 with an assumed $^{10}Be/^{9}Be$ value of $(26.8 \pm 1.4) \cdot 10^{-12}$. However, ^{10}Be production rates are usually referred to ICN standards, which assume $t_{1/2} = 1.52$ Ma, whereas the NIST standard assumes $t_{1/2} = 1.33$ Ma. We therefore systematically normalized to ICN standards the measured concentrations indexed on NIST by multiplying the latter by a factor of 1.143, after Middleton et al. (1993). ^{10}Be uncertainties incorporate a conservative estimate of 3% instrumental uncertainty, with lower than usual 1 sigma uncertainties associated with counting statistics due to high intrinsic boron contents that forced to reduce the AMS ion beam intensities. This affects age precision but not age accuracy. ^{10}Be ages are not corrected for magnetic field fluctuations over the investigated time span but their uncertainties integrate a 6% uncertainty on production rate.

Results

Results are summarized in Table 1 and represent exposure ages calculated for conditions of no erosion since exposure. Figure 6 shows a good coherence of ^{10}Be results, particularly when only the older boulder ages on moraines are considered (Putkonen and Swanson, 2003). The data define several key moments of the MIE and recessional stages of the last glaciation (Figs. 4 and 5). The MIE unit, which combines sites A and B, was followed by a first recessional stage (Borde unit, which combines sites C, D and E) situated only 3 km upstream from the MIE site. The later stages of ice retreat are defined by the Bouillouse–Grave unit (sites F, G, L, M, N and O) along the main Têt ice way, and by the Llat unit (sites H, I, J, and K) on the plateau. The anomalously old ages at sites D and I are most likely a consequence of nuclide inheritance of local significance.

The process of exposure dating calls for the additional task of correlating the ages with an independent paleoclimatic time scale. Here we use the INTIMATE event stratigraphy derived from the GRIP ice core as a standard proposed for NW Europe (Björck et al., 1998; Walker et al., 1999; Lowe et al., 2001; Johnsen et al., 2001). Overall, the east-Pyrenean chronology matches global temperature curves such as reconstructed from the GRIP ice core (Fig. 6). Results indicate that the MIE in the

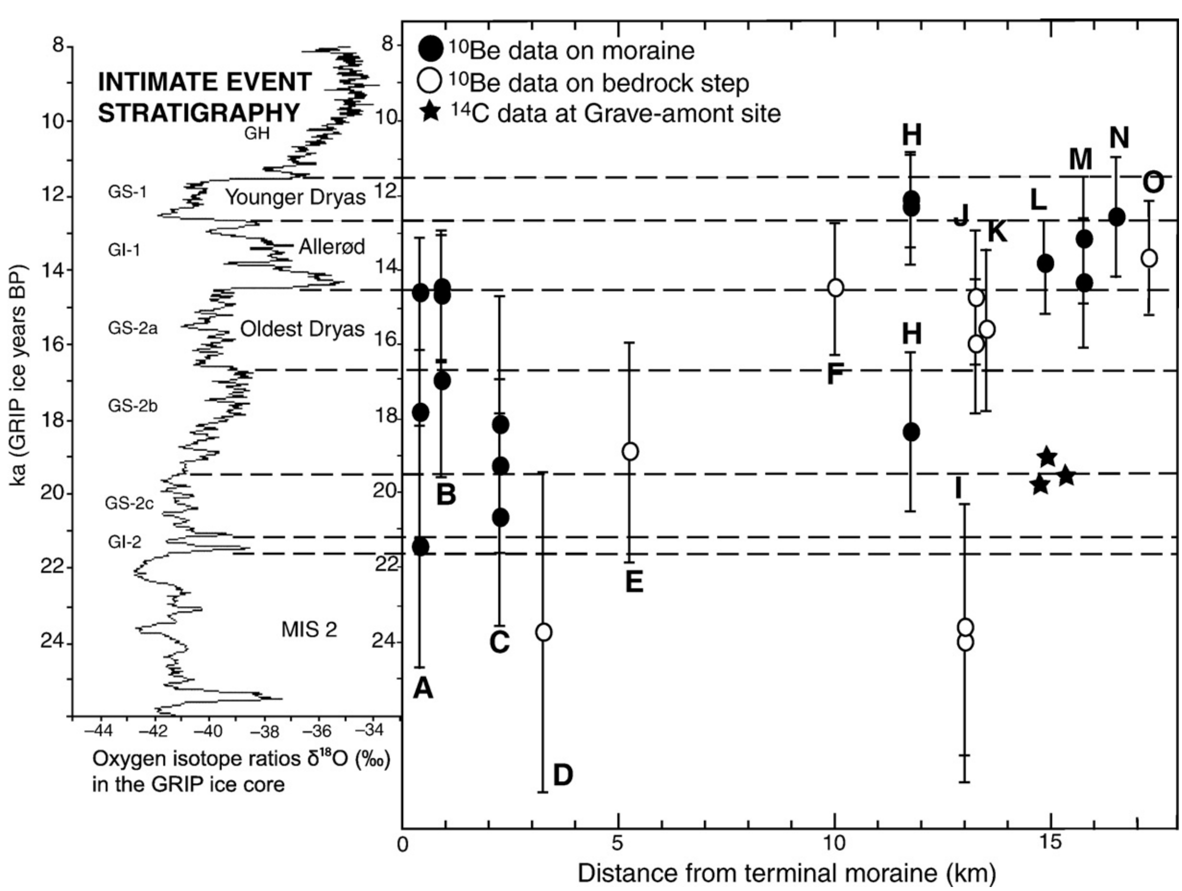

Figure 6. Tentative correlation between the ^{10}Be exposure age deglaciation chronology in the eastern Pyrenees and North Atlantic paleotemperature oscillations derived from the GRIP ice core chronology (based on Johnsen et al., 2001). Lower $\delta^{18}O$ values correlate with relatively warmer conditions.

eastern Pyrenees is synchronous with the North Atlantic LGM and MIS 2. Post-MIE deglaciation was interrupted around 20–21 ka (age for sample C3), i.e., during stage GS-2c of the INTIMATE nomenclature, by a phase of ice stagnation or even readvance (Borde unit, Fig. 5). This is consistent with the Borde units being located only 2–3 km from the MIE moraines. Deglaciation accelerated after GS-2c. This is clearly detectable in the Llat unit, where 14–15 ka ages on bedrock steps J and K suggest that the ice cap had receded to the mouths of existing cirques by the beginning of the Allerød interstade after a stage of stagnation or readvance detected around 17–18 ka (sample H2). This corresponds to the Oldest Dryas stade, i.e., GS-2a on the INTIMATE curve. Along the Têt ice stream, post-GS-2c retreat was more limited because a 5- to 8-km-long ice tongue still reached Les Bouillouses at the beginning of the Allerød interstade so that bedrock step F was exposed only after 13–14 ka. Despite their occurrence along an 8-km longitudinal stretch of the upper Têt valley between Les Bouillouses and La Grave, the closely matching ^{10}Be ages at sites F, L, M, N and O suggest rapid ice retreat during the warmer Allerød interstade. The 11.2 ± 1.9 ka age on moraine at the most elevated site O could indicate the persistence until the Younger Dryas stade (GS-1) of a cirque glacier in this uppermost reach of the Têt valley.

Discussion

The MIE ages obtained here for the eastern Pyrenees coincide with the timing of the MIS 2 LGM but do not match existing chronologies for other parts of the Pyrenees (see introductory overview). The MIE occurred much later than farther west, where it coincided with MIS 4 or 3 (see introductory section). Explanations for this may lie with discrepancies between chronologies indexed on different cosmogenic nuclides such as ^{10}Be and ^{14}C (see Pallàs et al., 2006), but here we suggest that this could be due instead to conditions specific to the eastern Pyrenees, namely the drier Mediterranean climate where Têt valley glaciers never exceeded 20 km in length. It could also be that the response of small glaciers to global forcing parameters may be more immediate than that of larger ice fields such as those of the central Pyrenees. The MIS 2 global thermal minimum would have thus triggered a sufficiently rapid expansion of the Carlit ice field for it to reoccupy a position formerly occupied during MIS 3 and 4.

The ^{10}Be chronology also suggests rapid post-Borde stage ice retreat, with deglaciation peaking during the Allerød interstade, i.e., at 14–13 ka. The rate of deglaciation during that time both in the upper valley at La Grave and among the Llat units is entirely in keeping with independent paleoenvironmental data for the eastern Pyrenees. Pollen studies in particular show that the timberline fell from 1.7–1.8 km a.s.l. during the Allerød interstade to 1.3 km a.s.l. during the Younger Dryas stade (Reille and Andrieu, 1993), and reached its current elevation of 2.2 km a.s.l. between 12,000 and 11,000 cal yr BP (Guiter et al., 2005). If we transpose to the Carlit massif the elevation difference of 1000 m between the glacier equilibrium and timberlines currently observed in the central Pyrenees, where residual glaciers still occur (Fig. 1), these data would suggest that all Carlit glaciers had definitively melted by the Allerød interstade. On that basis, it is unlikely that cirque glaciers survived at sites O or N much later than the Allerød interstade (Fig. 6).

Despite the relative simplicity of this single-nuclide chronology, matters are made somewhat more complicated by the existence of three ~20,000 cal yr BP radiocarbon ages recently obtained from a fossil peat bog situated at 2.15 km a.s.l. at the mouth of the cirques in the upper Têt valley. At this site, known as La Grave-amont (Delmas, 2005, see Figs. 1, 3, 5 and 6 and Electronic Supplement for full data), dating was performed on sphagnum fibre collected from *in situ* sphagnum layers after thorough washing for removal of fine mineral dust. X-ray diffraction analysis revealed a total absence of either graphite or carbonates within the peat. This rules out that the ages obtained might be artificially old due to a hard water effect or to the presence of graphite from Ordovician schists that are locally present within the catchment. Given that the peat could not have formed beneath ice, the existence and age of this peat bog suggest that ice had retreated to a position situated upstream of the Grave-amont site as early as GRIP-stage GS-2b (i.e., ~20,000 cal yr BP). A comparable deglaciation chronology has been reported from the Alps, where ice melt-out occurred during the same time intervals with ice retreat covering distances one order of magnitude greater than in the Têt basin. For instance, the MIE ^{10}Be age obtained for the terminal moraine of the Rhône glacier was 21 ka (Ivy-Ochs et al., 2004). That moraine is located ~100 km downstream of a recessional moraine equivalent to the Gschnitz stage (Austria), which has coeval occurrences in many high valleys of the Swiss and Austrian Alps and correlates with Heinrich event 1 (i.e., Oldest Dryas stade, immediately after GS-2b) on the basis of CRN ages obtained at Gschnitz (Ivy-Ochs et al., 2005, 2006).

GS-2b is known to have coincided with sharp ecological changes in the European Alps (Schoeneich, 2003) and with the first known signs of Magdalenian settlements in the northern French Alps (Bintz and Evin, 2002). Based on just one Pyrenean and one Alpine example, it would be bold at this stage to suggest that deglaciation in European mid-latitude mountain ranges occurred generally earlier (i.e., GS-2b) than previously believed. Despite mounting evidence in support of this claim, local conditions specific to the Carlit massif can nevertheless be used here as an alternative to explain the rapid retreat of ice as early as 20 ka. Firstly, the drier Mediterranean climatic overtones of the eastern Pyrenees differ from other parts of the Pyrenean range and are reflected in the smaller extent of glaciation and shorter glacier tongues despite only slightly lower elevations (Fig. 1). Secondly, the Carlit ice cap covered a pre-glacial (Cenozoic) plateau topography at ~2.2 km a.s.l. (Fig. 2) upon which the summit peaks and their cirques stand as residual relief of comparatively limited extent. The U-shaped Têt valley incising the plateau is ~0.3 km deep, and the plateau surface extends only 0.2 km above the MIE equilibrium line altitude (ELA, Delmas, 2005). As a result, just a small rise in ELA would have melted a disproportionately vast area of ice initially covering the plateau surface, and thus caused a major disequilibrium in the ice mass balance. Subglacial topography was therefore a source of nonlinearity in the rate of glacial retreat. Thirdly, the rapidity of ice wastage is further explained by the aridity of stage GS-2, which is documented regionally by pollen assemblages (Andrieu et al., 1988; Jalut et al., 1992).

The ^{14}C-driven hypothesis of a landscape deglaciated as early as stage GS-2b might appear to be at odds with the ^{10}Be data obtained for sites F, L, M, N and O of the Bouillouse–Grave unit, and sites H, J, K and I of the Llat unit. However, a reconciliation between the ^{14}C and ^{10}Be data can be envisaged if we consider the occurrence of a significant glacier readvance during the Oldest Dryas stade (i.e., GS-2a, which correlates with the Alpine Gschnitz stage). Based on the ^{10}Be results, this readvance would have progressed over the Llat area at least as far as moraine H (Fig. 2e). The readvance, however, was brief and apparently unable to reset ^{10}Be inheritance on some bedrock exposures such as I. Along the main Têt ice stream, the ^{10}Be ages for sites L and F indicate that this Oldest Dryas ice advance covered a distance of 5 to 8 km (Fig. 2c to e).

The hypothesis of an Oldest Dryas stadial readvance (GS-2a) remains the scenario most compatible with both the ^{14}C and ^{10}Be data, but one caveat regarding this reconstruction is that it fails to explain why the geologic record of its occurrence at the Grave-amont site is sedimentologically ambiguous. Based on the heights of preserved lateral and frontal moraines, such a GS-2a readvance would imply that a 100-m-thick ice tongue overrode the ~20,000 cal yr BP-old peat without any observable marks of erosion or compaction (e.g., the peat is sufficiently soft to be cut out with a pocket knife, as it would be in a surface environment). The peat is covered by a sequence initially consisting of lacustrine clays, which grade upward into a sandy deltaic facies, and are finally capped by an unconsolidated unit consisting of pebbles and large cobbles up to 50 cm in a-axis length and embedded in a sandy to gravelly matrix (Supplementary Fig. 1). Such a stratigraphy could suggest that the peat was buried by subglacial lodgment till deposited by a glacier advancing over its own proglacial lake deposits, and this null hypothesis would support the Oldest Dryas stadial readvance scenario (see above).

However, grain size distribution of the matrix material indicate that this diamicton is 25–50% poorer in clay-, silt-size and fine sand particles, and therefore better sorted, than other glacial till deposits in the area (Calvet, 1996). This could fit one of the characteristics of subglacial melt-out till (warm stagnant glacier or stagnant zone beneath an advancing glacier), which can sometimes show a relative depletion of fine material due to leaching by escaping porewater (Benn and Evans, 1998). However, clast a-axes are inclined upstream in a manner reminiscent of torrential facies architectures at other sites in the region. Finally and crucially, the top of this flat, gently sloping depositional formation connects topographically with moraine M situated <100 m upstream. The tread of this depositional landform is embayed in the moraine, and therefore cross-cuts it, at the point where the stream breaches the moraine (Supplementary Fig. 1). The Grave-amont landform unit seems therefore to correspond instead to a small glacio-fluvial fan that covered a shallow (<1.5 m paleodepth) proglacial lake at the snout of a receding glacier positioned close to site M. The lake was dammed by a small moraine situated immediately downstream (Supplementary Fig. 1). There is no additional evidence to support that this matrix-supported glacio-fluvial formation might itself have been covered by subglacial till that was later stripped.

To summarize, the hypothesis of a substantial glacial readvance, i.e., as far as the Bouillouses–Llat units, during the Oldest Dryas stade is in most part supported by the ^{10}Be data and the internally consistent sampling strategy that underpins it at the catchment scale, but it is challenged by our current understanding of stratigraphic and other evidence at the Grave-amont site. Consequently, the Grave-amont moraine (site M) can be interpreted in two ways: either it corresponds to an Allerød or Younger Dryas recessional stage of the Oldest Dryas readvance, which would imply that the ^{10}Be ages of the Bouillouse–Llat units are robust with respect to the deglaciation chronology, and that a 100-m-thick ice tongue advanced over the peat bog without any clear record of it in the stratigraphy. Or, alternatively, the Grave-amont moraine M is itself the front of the Oldest Dryas glacial readvance of the Têt glacier, in which case this cirque glacier never readvanced over the peat bog after GS-2b and never reached the more distal positions proposed in the previous scenario. In this case, it would have to be accepted that the Allerød interstadial ^{10}Be ages obtained for sites F, L, M and N are not true exposure ages but are biased by local environmental parameters such as delayed local exhumation of the bedrock steps from an overlying deposit, or post-depositional exhumation of moraine boulders. There currently exists no definitive evidence to separate these two hypotheses from one another. In suitable circumstances, it should for instance be possible to check for cases of nuclide inheritance (and hence non-erosive ice) on bedrock steps by comparing ^{10}Be concentrations on the surface with those measured on an erratic boulder resting on that same surface (e.g., Briner et al., 2003). Further dating of the Grave-amont lake deposits could also refine our understanding of the chronology of deglaciation in the eastern Pyrenees during the last glacial cycle.

Conclusions

The chronologic interpretation of ^{10}Be exposure ages is not direct because they provide minima, and not closure ages. Due to this, correlating ^{10}Be ages with a stratotype (e.g., GRIP) provides scope for tying a landform to an independently recognized stadial or interstadial although error bars, which for a range of reasons may exceed the wavelength of MIS wiggles, can be a limiting factor that makes ^{10}Be dating better suited to capturing lower frequencies fluctuations in climate. Together, these points explain why the chronologic value of the ^{10}Be data in this study is clearest at the two extremities of the chronosequence: the MIE and the cirque stage. Key conclusions are that the last east-Pyrenean MIE is recent, synchronous with the global LGM (i.e., MIS 2), and that deglaciation occurred over a 3–4 ka time span. A brief ‘neoglaciation’ may have occurred during the Oldest Dryas stade but ice, if at all present, had retreated to positions higher than 2.4 km a.s.l. by the Allerød interstade.

https://doi.org/10.1016/j.yqres.2007.11.004 Published online by Cambridge University Press

The exposure age chronology for the Oldest Dryas 'neoglaciation' stade in the eastern Pyrenees leads to two equally coherent competing hypotheses. In order to meet independent constraints provided by other data such as a radiocarbon-dated peat bog, each of the two hypotheses logically dictates that a small (but each time different) contingent of ^{10}Be data points needs to be considered as anomalous. Typical environmental factors leading to anomalous exposure ages are nuclide inheritance or retarded exhumation of sampled rock surfaces. The two competing scenarios permitted by the data highlight a recurring methodological problem with single-nuclide exposure dating; namely that the accuracy of ^{10}Be dating as a tool for tracking glacial chronology and climatic change relies on the ability of its users to evaluate the relation between the exposure time of rock surfaces sampled over areas of only a few cm^2 and the ages of much larger erosional and depositional landforms. Although the landforms unequivocally and directly integrate the glacial dynamics, this may not systematically be the case for the locally sampled rock exposures. Beryllium dating of the latter may record a much more complex local history which is neither of relevance to the climatic chronology nor of much value to the geomorphic history. Here, prior geomorphological mapping provided a relative event chronology and allowed reasonable distinctions to be drawn between landforms that directly record the recession chronology, and sites that reflect a more complex, but not necessarily relevant, local history. The existence of a radiocarbon-dated site has also allowed ^{10}Be ages to be put in perspective and helped in the evaluation of which ^{10}Be ages best represent the glacier recession chronology.

Acknowledgments

This work was partly funded by the Institut National des Sciences de l'Univers 'Reliefs' program. We acknowledge Pierre Giresse for assisting with the XRD analysis of the peat, and thank Jaakko Putkonen and Fred Phillips for their thoughtful reviews of the manuscript.

Appendix A. Supplementary data

Supplementary data associated with this article can be found, in the online version, at doi:10.1016/j.yqres.2007.11.004.

References

Andrieu, V., 1987. Le paléoenvironnement du piémont nord-pyrénéen occidental de 27 000 BP au Postglaciaire : la séquence d'Estarrès (Pyrénées Atlantiques, France) dans le bassin glaciaire d'Arudy. Comptes-Rendus de l'Académie des Sciences, Série II 304, 103–108.

Andrieu, V., Hubschman, J., Jalut, G., Hérail, G., 1988. Chronologie de la déglaciation des Pyrénées françaises Dynamique de sédimentation et contenu pollinique des paléolacs : application à l'interprétation du retrait glaciaire. Bulletin de l'Association Française pour l'Étude du Quaternaire 34/35, 55–67.

Bakalowicz, M., Sorriaux, P., Ford, D.C., 1984. Quaternary glacial events in the Pyrenees from U-series dating of speleothems in the Niaux–Lombrives–Sabat caves, Ariège, France. Norsk Geografisk Tidsskrift 38, 193–197.

Benn, D.I., Evans, D.J.A., 1998. Glaciers & Glaciation. Arnold, London. 734 pp.

Bintz, P., Evin, J., 2002. Evènements bio-climatiques et peuplements du Tardiglaciaire au début de l'Holocène dans les Alpes du Nord françaises. Quaternaire 13, 279–287.

Björck, S., Walker, M.J.C., Cwynar, L.C., Johnsen, S.J., Knudsen, K.L., Lowe, J.J., Wolhfarth, B., Intimate Members, 1998. An event stratigraphy for the Last Termination in the North Atlantic region based on the Greenland ice-core record: a proposal by the INTIMATE group. Journal of Quaternary Science 13, 283–292.

Bordonau i Ibern, J., 1992. Els complexos glacio-lacustres relacionats amb el darrer cicle glacial als pirineus. Geoforma édiciones, Logroño 251 pp.

Bordonau, J., Vilaplana, J.M., Fontugne, M., 1993. The glaciolacustrine complex of Llestui (Central Southern Pyrenees): a key-locality for the chronology of the last glacial cycle in the Pyrenees. Comptes-Rendus de l'Académie des Sciences, Série II 316, 807–813.

Briner, J.P., Miller, G.H., Davis, P.T., Bierman, P.R., Caffee, M., 2003. Last Glacial Maximum ice sheet dynamics in Arctic Canada inferred from young erratics perched on ancient tors. Quaternary Science Reviews 22, 437–444.

Calvet, M., 1996. Morphogenèse d'une montagne méditerranéenne : les Pyrénées orientales. Mémoire BRGM 255, Orléans. 1177.

Calvet, M., 2004. The Quaternary glaciation of the Pyrenees. In: Ehlers, J., Gibbard, P. (Eds.), Quaternary Glaciations — Extent and Chronology, Part I: Europe. Elsevier, Amsterdam, pp. 119–128.

Chueca Cía, J., Julián Andrés, A., Saz Sánchez, M.A., Creus Novau, J., López Moreno, J.I., 2004. Responses to climatic changes since the Little Ice Age on Maladeta Glacier (Central Pyrenees). Geomorphology 68, 167–182.

Delmas, M., 2005. La déglaciation dans le massif du Carlit (Pyrénées orientales): approches géomorphologique et géochronologique nouvelles. Quaternaire 16, 45–55.

Dunne, J., Elmore, D., Muzikar, P., 1999. Scaling factors for the rates of production of cosmogenic nuclides for geometric shielding and attenuation at depth on slopes surfaces. Geomorphology 27, 3–11.

García-Ruiz, J.M., Valero-Garcés, B.L., Martí-Bono, C., González-Sampériz, P., 2003. Asynchroneity of maximum glacier advances in the central Spanish Pyrenees. Journal of Quaternary Science 18, 61–72.

Gellatly, A.F., Grove, J.M., Switsur, V.R., 1992. Mid-Holocene glacial activity in the Pyrenees. The Holocene 2, 266–270.

González-Sampériz, P., Valero-Garcès, B.L., Moreno, A., Jalut, G., García-Ruiz, J.M., Martí-Bono, C., Delgado-Huertas, A., Navas, A., Otto, T., Deboubat, J.J., 2006. Climate variability in the Spanish Pyrenees during the last 30,000 yr revealed by the El Portalet sequence. Quaternary Research. 66, 38–52.

Guiter, F., Andrieu-Ponel, V., Digerfeldt, G., Reille, M., de Beaulieu, J.-L., Ponel, P., 2005. Vegetation history and lake-level changes from the Younger Dryas to the present in eastern Pyrenees (France): pollen, plant macrofossils and lithostratigraphy from Lake Racou (2000 m a.s.l.). Vegetation History and Archeobotany 14, 99–118.

Hérail, G., Jalut, G., 1986. L'obturation de Sost (Haute-Garonne): données nouvelles sur le paléo-environnement de la phase de progression du glacier würmien dans les Pyrénées centrales. Comptes-Rendus de l'Académie des Sciences, Série II 303, 743–748.

Ivy-Ochs, S., Schafer, J., Kubik, P.W., Synal, H.A., Schluchter, C., 2004. Timing of the deglaciation on the northern Alpine foreland (Switzerland). Eclogae Geologicae Helvetiae 97, 47–55.

Ivy-Ochs, S., Kerschner, H., Kubik, P.W., Schluchter, C., 2005. Glacier response in the European Alps to Heinrich Event 1 cooling: the Gschnitz stadial. Journal of Quaternary Science 21, 115–130.

Ivy-Ochs, S., Kerschner, H., Reuther, A., Maich, M., Sailer, R., Schaefer, J., Kubik, P.W., Synal, H.A., Schlüchter, C., 2006. The timing of glacier advances in the northern European Alps based on surface exposure dating with cosmogenics ^{10}Be, ^{26}Al, ^{36}Cl, and ^{21}Ne. In: Siame, L., Bourlès, D.L., Brown, E.T. (Eds.), In Situ-Produced Cosmogenic Nuclides and Quantification of Geological Processes. Geological Society of America Special Paper, 415, pp. 43–60.

Jalut, G., Andrieu, V., Delibrias, G., Fontugne, M., Pagès, M., 1988. Paleoenvironment of the valley of Ossau (Western French Pyrenees) during the last 27,000 years. Pollens et Spores 30, 357–394.

Jalut, G., Montserrat, J., Fontugne, M., Delibrias, G., Vilaplana, J.M., Julia, R., 1992. Glacial to interglacial vegetation changes in the northern and southern

Pyrenees: deglaciation, vegetation cover and chronology. Quaternary Science Reviews 11, 449–480.
Jiménez Sánchez, M., Farias Arquer, P., 2002. New radiometric and geomorphologic evidences of a last glacial maximum older than 18 ka in SW European mountains: the example of Redes Natural Park (Cantabrian mountains, NW spain). Geodinamica Acta 15, 93–101.
Johnsen, S.J., Dahl-Jensen, D., Gundestrup, N., Steffensen, J.P., Clausen, H.B., Miller, H., Masson-Delmotte, V., Sveinbjörnsdottir, A.E., White, J., 2001. Oxygen isotopes and palaeotemperature records from six Greenland ice-core stations: Camp Century, Dye 3, GRIP, GISP2, Renland and North GRIP. Journal of Quaternary Science 16, 299–307.
Lowe, J.J., Hoek, W.Z., Intimate Group, 2001. Interregional correlation of palaeoclimatic records for the Last Glacial–Interglacial Transition: a protocol for improved precision recommended by the INTIMATE project group. Quaternary Science Reviews 20, 1175–1187.
Mardonnes, M., Jalut, G., 1983. La tourbière de Biscaye (alt. 409 m, hautes Pyrénées) : approche paléoécologique des 45 000 dernières années. Pollen et Spores 25, 163–211.
Martí-Bono, C., González-Sampériz, P., Valero-Garcès, B., García-Ruiz, J.M., 2002. El depósito glaciolacustre de Linás de Broto (Pirineo aragonés) y su implicación paleoambiental. In: Pérez-González, A., Vegas, J., Machado, M.J. (Eds.), Aportaciones a la Geomorfología de España en el Inicio del Tercer Milenio. Actas de la VI Reunión Nacional de Geomorfologia: Madrid, 17–20 semtembre 2000, 1. Publicaciones del instituto geológico y minero de españa, serie: Geología, Madrid, pp. 77–83.
Middelton, R., Brown, L., Dezfouly-Arjomandy, B., Klein, J., 1993. On ^{10}Be standards and the half-life of ^{10}Be. Nuclear Instruments Methods Physics Research B 82, 399–403.
Pallàs, R., Rodés, A., Braucher, R., Carcaillet, J., Ortuno, M., Bordonau, J., Bourlès, D., Vilaplana, J.M., Masana, E., Santanach, P., 2006. Late Pleistocene and Holocene glaciation in the Pyrenees: a critical review and new evidence from ^{10}Be exposure ages, south-central Pyrenees. Quaternary Sciences Reviews 25, 2937–2963.
Peña, J.L., Sancho, C., Lewis, C., McDonald, E., Rhodes, E., 2004. Datos cronológicos de las morrenas terminales del glaciar del Gállego y su relación con las terrazas fluvioglaciares (Pirineo de Huesca). In: Peña, J.L., Longares, L.A., Sánchez, M. (Eds.), Geografia Física de Aragón. Aspectos generales y temáticos. Universitad de Zaragoza e Institución fernando el Católico, Zaragoza, pp. 71–84.
Putkonen, J., Swanson, T., 2003. Accuracy of cosmogenic ages for moraines. Quaternary Research. 59, 255–261.
Reille, M., Andrieu, V., 1993. Variations de la limite supérieure des forêts dans les Pyrénées (France) pendant le Tardiglaciaire. Comptes-Rendus de l'Académie des Sciences, Série D 272, 3112–3115.
Reille, M., Lowe, J.J., 1993. A re-evaluation of the vegetation history of the eastern Pyrenees (France) from the end of the last glacial to the present. Quaternary Science Reviews 12, 47–77.
Reille, M., Andrieu, V., 1995. The late Pleistocene and Holocene in the Lourdes basin, Western Pyrenees, France: new pollen analytical and chronological data. Vegetation History and Archaeobotany 4, 1–21.
Sancho, C., Peña, J.L., Lewis, C., McDonald, E., Rhodes, E., 2003. Preliminary dating of glacial and fluvial deposits in the Cinca River Valley (NE Spain): chronological evidences for the Glacial Maximum in the Pyrenees? In: Zapata, M.B., et al. (Ed.), Quaternary Climatic Changes and Environmental Crises in the Mediterranean Region. Universidad de Alcalá de Henares, pp. 169–173.
Schildgen, T.F., Phillips, W.M., Purves, R.S., 2005. Simulation of snow shielding corrections for cosmogenic nuclide surface exposure studies. Geomorphology 64, 67–85.
Schoeneich, P., 2003. Que s'est-il passé pendant la première partie du Tardiglaciaire? Indices d'un changement écologique majeur dès 17–18.000 cal BP. Preistoria Alpina 39, 9–17.
Sorriaux, P., 1981. Etude et datation de remplissages karstiques : nouvelles données sur la paléogéographie quaternaire de la région de Tarascon (Pyrénées ariégeoises). Comptes-Rendus de l'Académie des Sciences, Série II 293, 703–706.
Stone, J.O., 2000. Air pressure and cosmogenic isotope production. Journal of Geophysical Research 105, 23753–23759.
Taillefer, F., 1969. Les glaciations des Pyrénées. In : Actes VIII° congrès international INQUA, Bulletin de l'Association Française pour l'Etude du Quaternaire, Supplement, pp. 19–32.
Turu i Michels, V., 2002. Análisis secuencial del delta de Erts. estratigrafía de un valle glaciar obturado intermitentemente. Relación con en último ciclo glaciar. Valle de Arinsal, Pirineos Orientales. In: Estudios recientes (2000–2002) en geomorfología, patrimonio, montaña y dinámica territorial, SEG—Departamento de geografía UVA, Valladolid, pp. 555–574.
Viers, G., 1968. La carte du relief glaciaire des Pyrénées. Feuille de Mont-Louis au 1/50,000e (Pyrénées orientales). Revue Géographique des Pyrénées et du Sud-Ouest 39, 429–434.
Vilaplana, J.M., 1983. Quaternary Glacial Geology of Alta Ribagorça basin (central southern Pyrenees). Acta Geologica Hispanica 18, 217–233.
Vilaplana, J.M., Bordonau, J., 1989. Dynamique sédimentaire lacustre de marge glaciaire : le paléolac de Llestui (Noguera Ribagorçana, Versant sud des pyrénées). Bulletin de l'Association Française pour l'Étude du Quaternaire, 40, pp. 219–224.
Walker, M.J.C., Björk, S., Lowe, J.J., Cwynar, L., Johnsen, S., Knudsen, K.L., Wohlfarth, B., Intimate Group, 1999. Isotopic 'event' in the GRIP ice-core: a stratotype for the Late Pleistocene. Quaternary Science Reviews 18, 1143–1150.
Zreda, M.G., Phillips, F.M., 1994. Cosmogenic ^{36}Cl accumulation in unstable landforms. Water Resources Research 30, 3127–3136.